Conformation of End-Tethered PNIPAM Chains in Water and in Acetone by Neutron Reflectivity

H. Yim, M. S. Kent,* and D. L. Huber

Departments 1851 and 1122, Sandia National Laboratories, Albuquerque, New Mexico

S. Satija

National Institute of Standards and Technology, Gaithersburg, Maryland

J. Majewski and G. S. Smith

LANSCE, Los Alamos National Laboratories, Los Alamos, New Mexico

Received October 2, 2002

ABSTRACT: Poly(*N*-isopropylacrylamide) is perhaps the most well-known member of the class of temperature responsive polymers. It has a lower critical solution temperature (LCST) in water at about 32 °C. This very sharp transition (∼5 °C) is attributed to alterations in the hydrogen-bonding interactions of the amide group. In this work we investigated the conformation of end-tethered PNIPAM chains at the interface of silicon with D_2O and d-acetone using neutron reflection. End-tethered PNIPAM layers were prepared utilizing the interaction between COOH-terminated PNIPAM and OH-terminated self-assembled monolayers ("method A") and also by polymerizing *N*-isopropylacrylamide monomers from the silicon surface ("method B"). Reflectivity data from the protonated layers in deuterated water were obtained using a liquid cell over a range of temperature from 10 to 55 °C. For method A, PNIPAM molecular weights of 33K and 220K were examined. In D_2O, we observed very limited change in the conformation of the tethered chains as the temperature increased through the LCST. No conformational change was detected for the lowest molecular weight PNIPAM−COOH sample (33K). Only a slight change in conformation with temperature was detected for the higher molecular weight sample (220K) and the sample from method B. The profiles indicated that the chains were well hydrated above 32 °C, consistent with the observation of very low receding water contact angles. On the other hand, a significant change in the segment concentration profiles occurred when D_2O was replaced by d-acetone. Bilayer profiles were observed for all samples in D_2O. By contrast, in d-acetone the profiles were composed of a single monotonically decaying layer. Surprisingly, the profiles were more contracted in d-acetone than in D_2O despite the fact that PNIPAM dissolves in d-acetone but solutions of PNIPAM in D_2O are cloudy above the LCST. This observation, as well as the lack of conformational change with temperature for these low surface density brushes in D_2O, is explained on the basis of a concentration-dependent Flory χ parameter.

Introduction

Poly(*N*-isopropylacrylamide) (PNIPAM) exhibits a lower critical solution temperature (LCST) of ∼32 °C that is attributed to alterations in the hydrogen-bonding interactions of the amide group.[1−4] Gels of PNIPAM display remarkable hydration−dehydration changes in aqueous solution in response to relatively small changes in temperature (*T*). At temperatures lower than 32 °C PNIPAM gels hydrate to form an expanded structure, whereas they dehydrate at temperatures above 32 °C. Changes in volume of a factor of 10 have been reported.[5] Grafting PNIPAM to surfaces is a promising strategy for creating responsive surfaces, since the physical properties of PNIPAM are readily controlled by changing the temperature. PNIPAM in various forms has been explored for a variety of applications including controlled drug delivery,[6,7] solute separation,[8,9] tissue culture substrates,[10,11] and controlling the adsorption of proteins,[12] blood cells,[13] and bacteria.[14]

Considerable effort has been devoted to characterizing conformational changes in PNIPAM-based materials. In general, conformational changes play an important role in a wide variety of polymeric systems, including protein folding[15] and DNA packing.[16] Since polymer gels are of considerable practical importance and also represent a very convenient system to investigate this transition on a macroscopic level, many studies of the volume change of PNIPAM gels with temperature have been reported.[5,17−20] On the other hand, it is rather difficult to observe conformational changes in isolated polymer chains through the transition temperature because of interchain aggregation.[21−23] Wu et al. studied the conformational change of PNIPAM chains with high molecular weight and low polydispersity ($M_w = 1.3 \times 10^7$ g/mol, $M_w/M_n < 1.05$) in an extremely dilute aqueous solution using laser light scattering.[21,22] They found that the radius of gyration (R_G) decreased by a factor of 7 as the solution temperature increased above the LCST.

There have been few direct experimental studies of the conformational changes of end-tethered PNIPAM chains. Kidoaki et al. recently reported changes in the thickness of a chemically grafted PNIPAM layer in an aqueous solution using AFM.[24] They employed an iniferter-based graft polymerization method[25] to generate PNIPAM films with dry thicknesses ranging from 250 to 1500 Å. Precise values of surface density (σ) and molecular weight (*M*) were not reported. The change in thickness of the grafted layer was estimated from AFM images of the boundary between grafted and nongrafted (ablated by laser light) regions. They found that the swollen film thickness decreased by a factor of ∼2 upon increasing the temperature from 25 to 40 °C.

10.1021/ma021548o CCC: $25.00
Published on Web 06/20/2003

A number of indirect methods that may be sensitive to conformational changes of grafted PNIPAM chains have also been reported. Several studies have been reported of the hydrodynamic radii of colloidal particles with grafted or adsorbed PNIPAM molecules.[26−29] Zhu and Napper studied the temperature dependence of the hydrodynamic radii of latex particles with grafted[26] and adsorbed[27] layers of PNIPAM by dynamic light scattering. For grafted layers with molecular weights from 3×10^5 to 2×10^6 g/mol, they found a strong decrease in the hydrodynamic radius (R_h) with increasing temperature through the LCST.[26] The range of surface density was not reported. NMR data supported the notion that two processes were involved in the transition, one dominating below 28 °C and one dominating above 28 °C. The authors assigned these processes to strong attractive binary interactions and weaker attractive many-body interactions. Whereas the contraction through the transition was very pronounced for all molecular weights, the authors concluded that the contributions of the two processes had opposite dependencies on molecular weight based on changes in the shape of the R_h vs T curves.

Takei et al. investigated the change of surface properties for PNIPAM grafted surfaces using dynamic contact angle measurements.[30] They observed a large change in advancing water contact angle with temperature and reported receding contact angles as high as 60°. On the other hand, others have reported little change in advancing contact angle with temperature and much lower receding contact angles.[24,31] For surfaces of grafted PNIPAM prepared by the iniferter technique, Kidoaki et al. reported advancing water contact angles of 64 ± 2.5° independent of temperature from 20 to 40 °C and receding contact angles that increased from 17.8 ± 1.7° to 33.8 ± 2.2° over this range for their highest molecular weight sample.[24] Schmitt et al. studied the temperature-dependent properties of layers of PNIPAM slightly copolymerized with a hydrophobic monomer adsorbed to mica from aqueous solution.[31] They found that the advancing contact angle was nearly constant from 20 to 35 °C and had an average value of $\theta_a = 76 \pm 2°$. The receding contact angle increased from 18° to 33° between 25 °C and 30 °C.

Theoretical understanding of grafted polymer chains is not nearly as advanced for LCST systems as for UCST systems.[32,33] Regarding layers of grafted PNIPAM chains, Baulin and Halperin recently proposed a phenomenological theory based on a concentration-dependent Flory χ parameter.[34] To explore the effect of a spatially varying segment concentration (ϕ) in this case, the brush was modeled in the Pincus approximation.[35] This approximation retains the uniform stretching assumption of the scaling approach of Alexander[36] but allows for spatial variation in ϕ and in the distribution of chain ends. For the generic case of $\chi = 0.5 + a\phi^2$, where $a \sim 1$, they obtained two types of behavior based on the surface density. For monodispersed chains at sufficiently high σ, a vertical phase separation within the brush resulted which led to a bilayer profile. On the other hand, for lower σ no such vertical phase separation occurred and single layer profiles resulted. Profiles were also calculated for grafted PNIPAM layers at 28 °C using experimental data for $\chi_{eff}(T,\phi)$ obtained from the recent study of PNIPAM phase behavior by Afroze et al.[37] This analysis resulted in bilayer profiles at high σ and single layer profiles at low σ. Behavior for the full range of temperature through the transition was not reported. Since this phenomenological approach incorporated $\chi_{eff}(T,\phi)$ obtained from macroscopic phase behavior, no connection was made to the nature of the fundamental interactions.

In this work we directly investigated the conformational changes of PNIPAM chains tethered to a flat substrate and immersed in water as a function of temperature using neutron reflection (NR). The PNIPAM chains were tethered by two methods. The first method ("method A") involved the association of end-functionalized preformed polymers with functional groups on the substrate, analogous to the "grafting-to" method[38−40] but without a covalent linkage. The other method ("method B") is the "grafting-from" method.[41−43] In general, higher surface density can be obtained using the second method as only small molecules have to diffuse to the surface, and blocking of binding sites by already tethered material is minimized. However, in the present work the surface density for this method, while greater than that for method A, was still rather low. Segment concentration profiles of the PNIPAM brushes were determined in D_2O as a function of temperature and also in d-acetone at room temperature. Profiles were obtained in the two solvents in order to investigate the role of the solvent in mediating interactions. Changes in water contact angles with temperature were also measured and are discussed below along with the concentration profiles. In both of the tethering methods used in this work, the dry film thickness was less than 40 Å, which is much lower than in the study of Kidoaki et al. We show below that, for the present range of surface density and molecular weight, the conformational changes are far more modest than reported in the study of Kidoaki et al. No coil-to-globule transition was observed. Many tethered PNIPAM systems fall into the present range of surface density and molecular weight. The present data imply that the mechanisms underlying various useful applications of PNIPAM for these cases do not involve large conformational changes. This is contrary to much previous speculation regarding such mechanisms.[4,13,30,44,45]

Experimental Section

Materials. Dodecyltrichlrosilane (DDTS), bromoundecyltrichlrosilane (BrUTS), and (3-mercaptopropyl)trimethoxysilane were obtained from Gelest.[46] Anhydrous hexadecane was obtained from Aldrich. Carboxylic acid-terminated PNIPAM with molecular weights of 33 000 and 220 000 g/mol were obtained from Polymer Source. The samples were fractionated from a polydisperse sample, and M_w/M_n was ∼1.4 for both samples. *N*-Isopropylacrylamide (NIPAM), *N*,*N*-dimethyltrimethylsilylamine (DMTMSA), D_2O (99.9 atom %), acetone-d_6 (99.9 atom %), and azobis(isobutyronitrile) (AIBN) were obtained from Aldrich. NIPAM was recrystallized from hexane; all other materials were used as received.

Methods. For the samples of method A, the silicon wafers were cleaned in a piranha solution (70/30 H_2SO_4/H_2O_2) and then submerged for 5 h in a hexadecane solution containing a mixture of DDTS and BrUTS at 60 °C.[47] The monolayer composition was controlled by varying the composition of the treating solution. For the data discussed below, the composition was 40 mol % BrUTS. The SAM-coated wafers were sonicated in toluene to remove nonbonded material and then blown dry with a stream of dry nitrogen. The conversion of Br termination to OH termination was accomplished following the procedure outlined by Baker and Watling.[48] PNIPAM films were then spin-coated from a 1 wt % methanol solution onto the mixed SAM-coated wafers. The thicknesses of the PNIPAM films were ∼400 Å, measured by ellipsometry. The wafers were

then annealed for 48 h in a vacuum oven at 150 °C to enable the carboxylic acid end groups to interact with the hydroxyls on the substrate surface. No change was detected in the IR spectrum of bulk PNIPAM exposed to the same conditions, indicating that PNIPAM does not degrade under these conditions. The samples were then submerged in a water bath at 5 °C for 2 weeks and also sonicated in an acetone bath. The thickness of the surface layer was measured by X-ray reflectivity (XR) before and after tethering the PNIPAM chains. The final dry film thickness of PNIPAM ranged from ∼10 to 40 Å for these samples. While many samples were prepared in this way and examined, in the following we discuss the data for two samples which we refer to as "33K" and "220K" according to their molecular weights. Evidence for end-tethering came from the fact that PNIPAM samples without COOH terminal groups could be completely rinsed off the same mixed SAM surfaces, but a substantial thickness was retained after exhaustive rinsing for the PNIPAM−COOH samples. The mode of association was most likely hydrogen bonding, as no evidence of ester formation was seen in an IR study of a bulk sample of PNIPAM−COOH in the presence of an excess of octanol under the same conditions.

The "grafting-from" sample (method B) was synthesized through a chain-transfer polymerization, where radicals were generated in solution and then transferred to the surface. The silicon wafer was first coated with (3-mercaptopropyl)trimethoxysilane (MPS), which functions as the chain-transfer agent, by submerging it for 2 min in a 2% silane solution in an ethanol/water mixture (20:1) acidified to pH 5.5 with acetic acid. After an ethanol rinse, the condensation was driven by heating at 110 °C for 10 min. The MPS-coated sample was then placed into a 25% NIPAM solution in dioxane with 20 mg/mL AIBN. The sample was heated to 60 °C under a nitrogen atmosphere and allowed to react for 20 h. The sample was rinsed exhaustively with room temperature 2-propanol to remove unbound polymer.

The neutron reflectivity (NR) measurements were performed on the NG7 reflectometer at NIST. A fixed wavelength of 4.75 Å was used. Reflectivity data from the protonated PNIPAM layers in deuterated water were obtained using a liquid cell over a range of temperature from 10 to 55 °C. Following that, the deuterated water in the liquid cell was removed and the cell was refilled with d-acetone. Reflectivity data for the sample in d-acetone were then collected at 20 °C. For PNIPAM brushes obtained by method A, neutron reflectivity data were also collected in the liquid cell (both solvents) after removing the PNIPAM brushes. The latter measurements served to determine the penetration of the solvents into the SAM layer and oxide and was used to constrain the fitting. The PNIPAM brushes were removed by depositing *N*,*N*-dimethyltrimethylsilylamine (DMTMSA) onto the sample surface for 15 min and then rinsing several times with methanol and acetone. The procedure was repeated twice. X-ray reflectivity was also performed on the dry films after removing the PNIPAM to verify complete removal. The ability to remove the layer completely with *N*,*N*-dimethyltrimethylsilylamine is consistent with the conclusion that the PNIPAM molecules were not covalently grafted to the OH-terminated SAM layer. Neutron reflection probes the scattering length density (SLD) profile normal to the surface, which is a function of the density and atomic composition. The SLD profiles were converted to volume fraction profiles assuming additivity of volumes. The SLD profiles were composed of a stack of slabs, where each slab was assigned an SLD, a thickness, and a roughness. The reflectivity was calculated from the stack of slabs using the optical matrix method.[49] Best-fit profiles were determined by minimization of least squares. X-ray reflectivity was performed both at SNL and at NIST. X-ray reflectivity determines the electron density profile normal to the surface.[50]

Advancing (θ_a) and receding (θ_r) water contact angles on selected samples were measured using the dynamic Wilhelmy plate technique and the sessile drop technique. For the former method, two pieces of silicon wafer coated with PNIPAM were prepared identically and then glued together so that PNIPAM-coated surfaces were exposed on both faces. Measurements were made with a Hottinger Baldwin Q11 load cell. The advancing and receding contact angles were measured at a speed of 10 mm/min for five consecutive cycles. Calculations of the dynamic contact angles were performed according to a procedure outlined by Smith and co-workers.[51] For the sessile drop method, a Kruss DSSA10 MKII system was used. The samples were enclosed in an environmental chamber and heated with a thin film resistance heater.

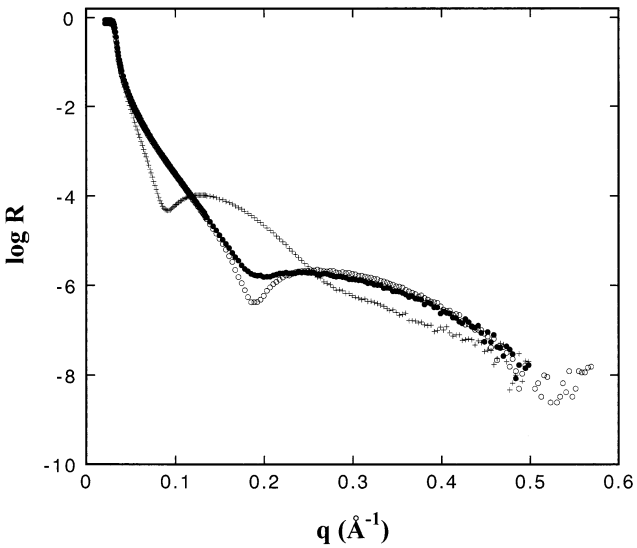

Figure 1. (a) X-ray reflectivity data for the 33K sample: SAM only (○), with PNIPAM (+), and after removing PNIPAM with DMTMSA (●).

Results

XR was used to measure the PNIPAM dry film thicknesses, which was important for constraining the fits to the NR data. An example is given in Figure 1, where data for the SAM layer alone, the SAM with tethered PNIPAM (33K), and the SAM layer after removal of the PNIPAM layer are shown. The first minimum shifted to lower q for the sample with PNIPAM, indicating a PNIPAM thickness of ∼10 Å. The surface coverage calculated from this thickness is ∼1.0 mg/m^2, assuming a density of 1.0 g/cm^3 for PNIPAM. After removing the PNIPAM layer with DMTMSA, the first minimum in the curve shifted back to the same position as obtained initially for the SAM layer alone, although the fringe was less distinct. This indicates near complete removal of the tethered PNIPAM chains by DMTMSA. We note that XR for the 33K and 220K samples in air was measured both before and after the NR measurements. Little change was observed for both samples, indicating that PNIPAM molecules were not removed during the NR experiments. Dry film thicknesses for the 220K PNIPAM−COOH sample (hereafter referred to as 220K) and the "grafting-from" sample were 56 Å and 43 Å, respectively, where the former includes an 18 Å SAM layer and the latter includes an 8 Å layer of mercaptopropyltriethoxysilane.

NR data for 33K and 220K in D_2O at 20 °C are shown in Figure 2a, along with data for a sample with the SAM only. Data for the same samples in d-acetone at 20 °C are shown in Figure 2b. The data are displayed as reflectivity × q^4 to compensate for the q^{-4} decay due to the Fresnel law. In this comparison, one can see a much larger change near the minimum in the curve after tethering in d-acetone than in D_2O. Since the neutron scattering contrast for PNIPAM is stronger in D_2O and than in d-acetone, the stronger signal in d-acetone

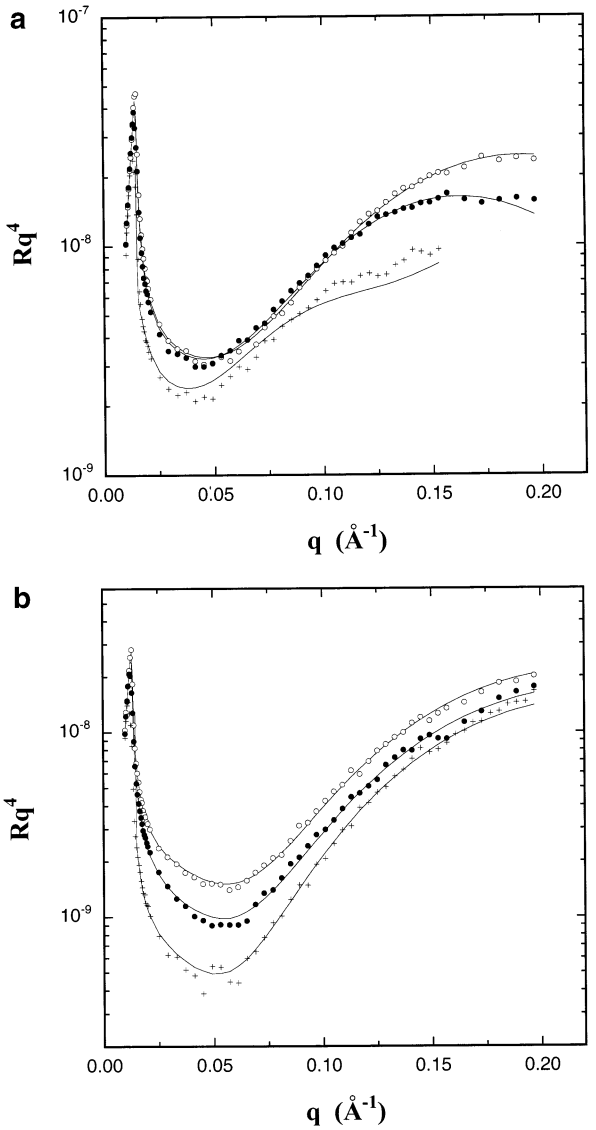

Figure 2. (a) Neutron reflectivity data for SAM only (○), 33K (●), and 220K (+) in D_2O. The curves through the data correspond to best fits. (b) Neutron reflectivity data for SAM only (○), 33K (●), and 220K (+) in d-acetone. The curves through the data correspond to best fits.

indicates, without detailed fitting, that the chains are more contracted in d-acetone than in D_2O. In D_2O the reflectivity for 33K deviates only slightly from that for the SAM layer alone, falling slightly lower at high q. This weak signal indicates that the PNIPAM layer is highly expanded. Whereas a detailed profile cannot be obtained, limitations on the profile shape, specifically the extent of contraction, can be determined since the mass of PNIPAM is known from XR. From this analysis we find that the layer must be more expanded than a layer of 170 Å with average segment volume fraction of 0.05, as this layer would produce a measurable difference from the reflectivity for the SAM alone in the range of $q = 0.02-0.05$ Å^{-1}. For all other cases, detailed profiles were obtained.

Figure 3a shows NR data for 33K in D_2O at 20 and 55 °C and in d-acetone at 20 °C. Surprisingly, no change in reflectivity was observed for 33K in D_2O as the temperature passed through the bulk LCST. Similarly, no change in reflectivity with temperature was observed

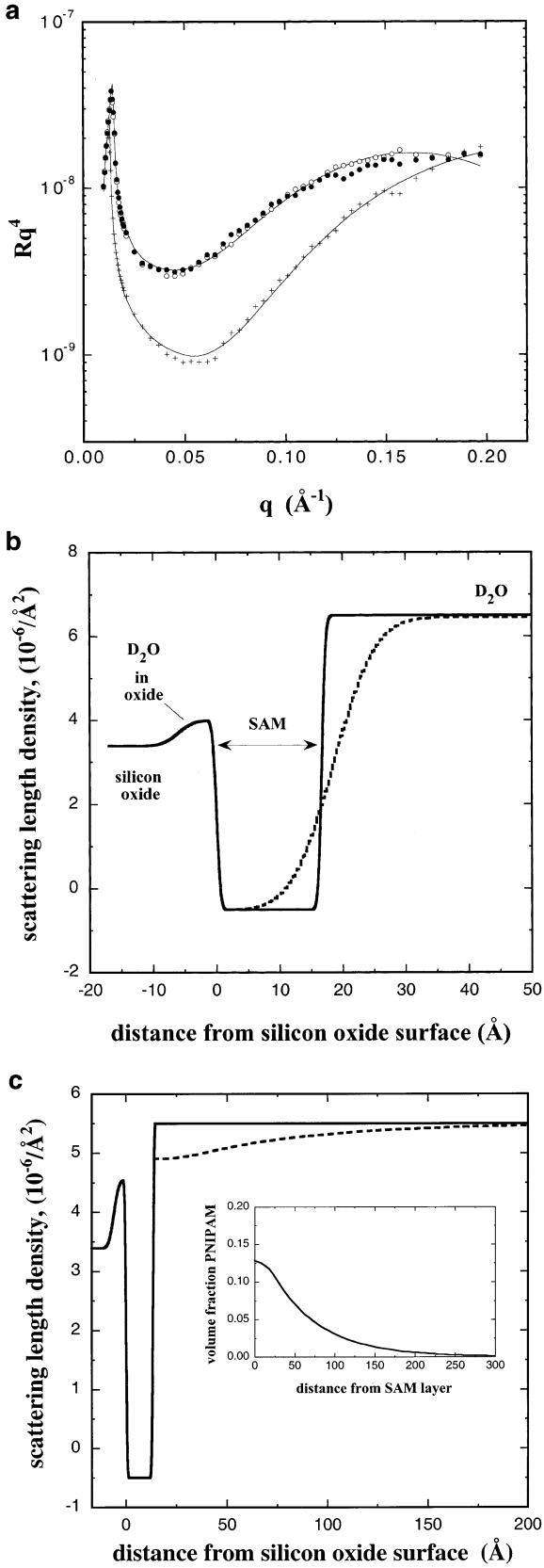

Figure 3. (a) Neutron reflectivity data for 33K in D_2O at 20 °C (○), in D_2O at 55 °C (●), and in d-acetone (+). The curves through the data correspond to best fits. (b) Best-fit SLD profiles for the 33K sample in D_2O (- - -) and the sample in D_2O after removal of PNIPAM with DMTMSA (—). (c) Best-fit SLD profiles for the 33K sample in d-acetone (- - -) and the sample in d-acetone after removal of PNIPAM with DMTMSA (—). The inset shows the PNIPAM segment concentration profile in d-acetone.

for other tethered PNIPAM samples with molecular weights ranging from 10 000 to 33 000 g/mol and for similar surface densities as for 33K in Figure 3a. The curves through the data in Figure 3a correspond to the SLD profiles shown in Figures 3b and 3c. We emphasize that the fits were highly constrained. The integral of the profile was constrained at the thickness obtained for the dry film by XR. Furthermore, the SLD and thickness values for the silicon oxide and SAM layers were fixed to values obtained from NR data for the SAM layer alone for both D_2O and d-acetone. We note that it was necessary to account for the presence of solvent within the oxide. A similar result was reported previously by Lu et al.[52] Comparable fitting results were obtained for either adding a thin layer (~5 Å) with an elevated SLD near the outer surface of the oxide or increasing the SLD of the oxide layer uniformly. As mentioned above, for 33K in D_2O the signal was very weak. A detailed SLD profile could not be obtained from this NR curve, but rather the curve could be fitted by simply increasing the roughness between the SAM and D_2O, as shown in Figure 3b. The appearance of penetration of solvent into the SAM layer in Figure 3b is an artifact of the one-dimensional SLD profile. This effect is due to an increased roughness parameter between the SAM and the subphase, likely stemming from in-plane heterogeneity of PNIPAM segments at the SAM surface. On the other hand, in d-acetone a significant signal was observed, and information about the profile could be obtained. A smoothly decaying single layer profile is adequate to describe the data.

Figure 4a shows NR data for 220K in D_2O at 20 and 55 °C and in d-acetone at 20 °C. For this sample in D_2O, there was a noticeable change in reflectivity over this temperature range. The curves through the data correspond to the segment concentration profiles shown in Figure 4b. For 220K in D_2O, the data are not consistent with a single layer profile. On the other hand, the data are consistent with a bilayer profile composed of a very thin layer of high concentration at the substrate surface followed by a second layer of much lower concentration which extends well into the subphase. The change in conformation of the PNIPAM chains in D_2O observed with temperature is complex. It does not simply indicate a contraction of one of the layers, but rather changes occur in both layers. We note that the reflectivity returned to that of the original curve upon subsequent decrease in temperature to 20 °C. Good reversibility was obtained for several heating−cooling cycles. In contrast to the profiles in D_2O, a bilayer profile is not required to fit the data for 220K in d-acetone, but rather the data are consistent with a smoothly decaying single layer profile. Similar to the results for the 33K sample, the 220K PNIPAM chains are more collapsed (rms thickness of segment concentration profile much smaller) in d-acetone than in D_2O.

Figure 5a shows neutron reflectivity data for the PNIPAM sample obtained using the "grafting-from" method in D_2O at 20 °C and 55 °C and in d-acetone at 20 °C. We expect the surface density to be higher for chains tethered by this method than with the other method (recall that only 40% of the surface area was terminated with OH in the mixed SAM of method A, whereas 100% of the surface area was coated with MPS in the "grafting-from" method). For this sample the dry film thickness of PNIPAM from XR was ~35 Å. A small but clearly measurable change in reflectivity was observed with increase in temperature to 55 °C. The best-fit segment concentration profiles are shown in Figure 5b. A smoothly decaying single-layer profile is again consistent with the data for the PNIPAM sample in d-acetone, whereas a bilayer profile is once more required in D_2O. However, the second layer is less distinct than for the 220K sample. Finally, we note that the change in reflectivity with temperature was not reversible upon cooling back to 20 °C for this sample.

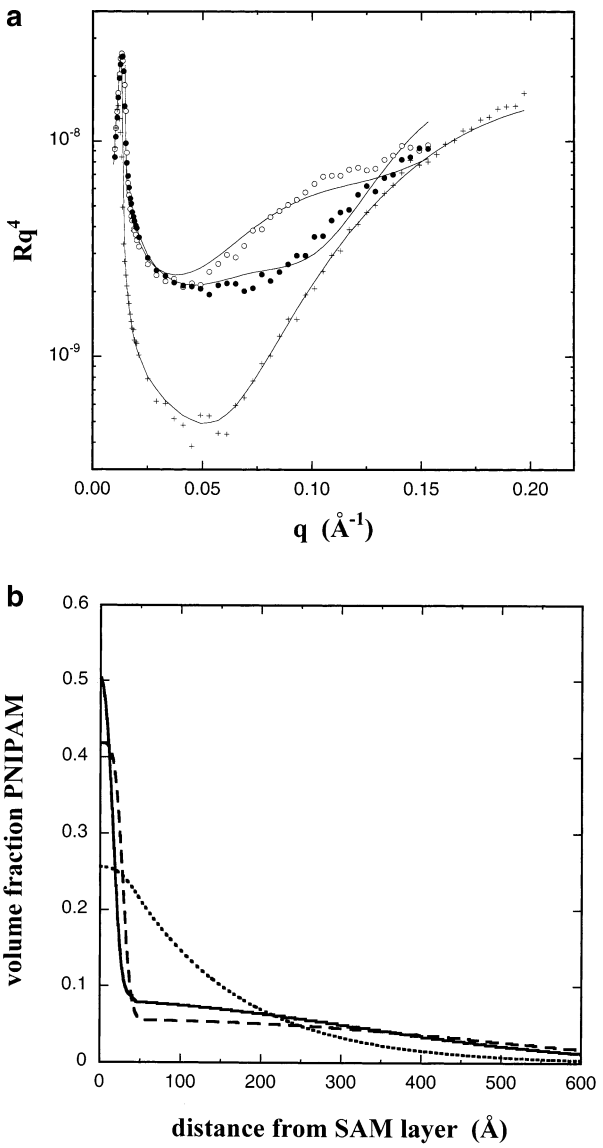

Figure 4. (a) Neutron reflectivity data for 220K in D_2O at 20 °C (○), in D_2O at 55 °C (●), and in d-acetone (+). (b) Best-fit segment concentration profiles for the sample in D_2O at 20 °C (—), in D_2O at 55 °C (- - -), and in d-acetone (···).

Advancing and receding water contact angles at 22 and 40 °C for 33K on 40% hydroxyl-terminated SAM are shown in Table 1. Whereas the values for the contact angles were roughly in the same range with each method, differences were observed in the temperature dependencies. With the dynamic Wilhelmy plate method, we observed only a small increase in advancing contact angle over this temperature range. A stronger increase with temperature was observed in the receding contact angle, but the values still remained quite low. For the sessile drop method, an increase of 19° was observed in

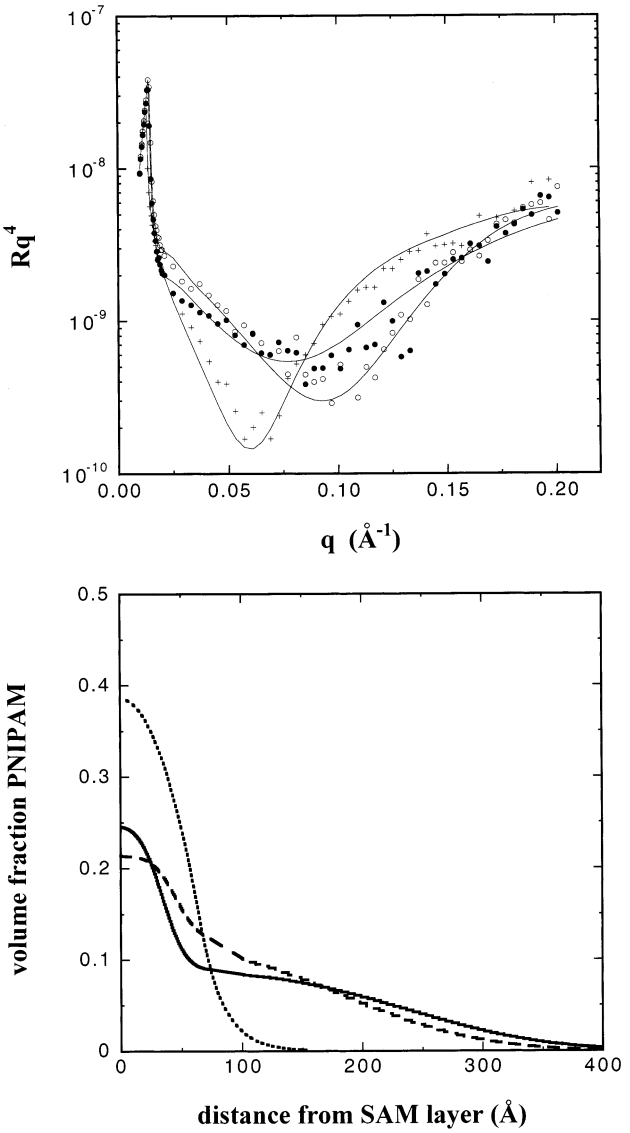

Figure 5. (a) Neutron reflectivity data for the "grafting-from" sample in D_2O at 20 °C (○), in D_2O at 55 °C (●), and in d-acetone (+). (b) Best-fit segment concentration profiles for the sample in D_2O at 20 °C (—), in D_2O at 55 °C (- - -), and in d-acetone (···).

Table 1. Water Contact Angles of 33K PNIPAM−COOH on 40% OH-Terminated SAM

PNIPAM sample	22 °C		40 °C	
	advancing	receding	advancing	receding
dynamic	79.4 ± 3.7	4.8 ± 4.8	87.4 ± 8.9	28.9 ± 2.0
Wilhelmy plate				
sessile drop	70.0 ± 1.4	17.9 ± 0.9	89.2 ± 2.5	18.1 ± 1.7

the advancing contact angle over this temperature range while the receding contact angle remained constant. Importantly, for both methods the receding contact angles were far below the receding contact angle obtained for the mixed SAM in absence of the PNIPAM film (∼70°). The very low receding contact angles demonstrate that these PNIPAM brushes are well solvated by water even above the bulk LCST. Our results are similar to the data of Schmitt et al. and Kidoaki et al. but contrary to the data of Takei et al., who reported much higher receding contact angles.

Discussion

The first important observation of this work is that, for the present range of σ and M, the change in conformation of the tethered PNIPAM chains is very subtle as the temperature increases above the LCST in D_2O. This result was obtained for both tethering methods. The lack of strong conformational change with temperature is striking given the fact that an aqueous solution of free chains undergoes a cloud point transition over the same temperature range. The concept of a concentration-dependent Flory χ parameter may provide insight into this observation. The surface density was relatively low for all the samples in the present study, as can be inferred from the segment concentration at the surface for the profiles in d-acetone. The very modest conformational changes observed in D_2O may be due to the fact that all the layers in this study fall into the low-density regime where attractive interactions between segments are weak. In support of this interpretation, we note that in more recent measurements to be reported elsewhere[53] involving brushes at much higher surface density a strong contraction with temperature was observed. We emphasize that the lack of observed change in the segment density profile with temperature in D_2O in the present work is not due to limited sensitivity of the experimental technique, as demonstrated by the fact that a substantial change in profile shape was detected upon replacing D_2O with d-acetone.

A second important observation of this study is the comparison between changing the temperature with D_2O vs replacing D_2O with d-acetone. We note that free PNIPAM has a UCST in d-acetone at ∼−56 °C and thus dissolves at all temperatures of this study. On the other hand, free PNIPAM dissolves in D_2O for $T < 32$ °C but precipitates from solution for $T > 32$ °C. Two striking differences are observed in the tethered chain profiles for the two methods of varying the solvent quality. First, the reflectivity data are consistent with a smoothly decaying single-layer profile in d-acetone, but a bilayer in D_2O. Second, the chains are more contracted in d-acetone than in D_2O at 55 °C, as measured by the rms thickness of the segment concentration profile. These two observations reveal the complex nature of the interactions in this system. In addition to surface density and molecular weight, many interactions are involved in determining the profile shape of grafted chains: solvent−substrate, segment−substrate, segment−solvent, and segment−segment interactions. Furthermore, since the NIPAM monomers possess both hydrophobic and hydrophilic moieties, their interaction with other segments, the solvent, or the surface must comprise a combination of very different types of interactions. Raising the temperature in D_2O presumably affects primarily the hydrogen-bonding interactions of the amide groups.[1−3] However, replacing D_2O with d-acetone affects all the interactions in the system. Thus, it is perhaps not surprising that replacing D_2O with d-acetone produces a larger conformational change in some cases than simply varying the temperature in D_2O. We speculate on the details of these interactions below, focusing first on the interactions with the surface and then turning to the interactions which control the extension of the tethered chains into the solvent.

Since there is little change in the profile with temperature in D_2O, the bilayer profiles are interpreted in terms of strong attractive interactions between PNIPAM chain segments and the SAM surface, rather than in

terms of a vertical phase separation as in the theory of Baulin and Halperin. The effect of surface interactions on the shape of segment concentration profiles for end-tethered and adsorbed chains has been investigated theoretically[54−58] and experimentally.[33,59−63] A depletion of segments from the surface is present for a neutral or repulsive segment−surface interaction, and an excess of segments is present for an attractive interaction. The magnitude of the excess is dependent upon the strength of the attraction. Experimentally, bilayer profiles have been previously reported for several systems with strong surface attraction, such as β-casein at the interface between water and a self-assembled monolayer of octadecyltrichlrosilane on silicon (hydrophobic interactions)[60] and poly(styrenesulfonate) adsorbed from aqueous solutions onto weakly charged polystyrene latex particles (electrostatic interactions)[61] or at the air surface of water (driven by difference in surface energy).[62] This contrasts with profiles reported previously for polystyrene (PS) chains end-grafted onto surfaces that are weakly attractive, neutral, or repulsive for the PS chains. Karim et al. studied PS grafted onto silicon oxide and immersed into cyclohexane with NR.[63] In that case the nonpolar PS interacts only weakly with the silicon oxide surface. The data were consistent with single layer profiles that decayed according to the prediction of self-consistent-field theory. In another study, the attraction of tethered polystyrene chains to a surface was varied from repulsive to slightly attractive using Langmuir monolayers of diblock copolymers on the surfaces of various organic solvents.[33] The surface energy of the solvent relative to that for PS determined the surface interaction. For the repulsive case, a depletion of segments was found at the surface followed by a smooth decay from the maximum. For the case of a mild attraction, the data were consistent with a profile composed of a step at the surface followed by a smooth decay.

In the present work, the bilayer profiles in D_2O indicate that the attraction of the PNIPAM segments to the substrate surfaces is apparently much stronger than in the above-mentioned two studies involving tethered PS. This can be explained by the presence of hydrophobic interactions between the isopropyl groups of the NIPAM segments and the surface in the present system. Whereas both tethering methods lead to bilayer profiles in D_2O, the shapes of the profiles are quite different. The distinct bilayer profiles for 220K, with a high volume fraction of PNIPAM segments in the surface layer, would seem to indicate a very strong attractive interaction between the segments and the surface. The lower concentration in the surface layer in D_2O for the "grafting-from" sample suggests a much weaker attraction. This could be due to chemical differences in the exposed surfaces of the substrates in the two cases. For the 220K sample, 60% of the sites on the mixed SAM are methyl-terminated, whereas 100% of the surface area was coated with MPS in the "grafting-from" method. Thus, hydrophobic interactions should be more predominant for the 220K sample.

The single-layer profiles found for the PNIPAM chains in d-acetone indicate a much weaker net attraction of the segments to the substrate surface than in D_2O. The profiles in d-acetone are similar to those observed for a mild attraction to a tethering surface.[33] Hydrophobic interactions could explain much stronger segmental adsorption in D_2O than in d-acetone. Thus, the comparison of the profile forms in D_2O and in d-acetone suggests that solvent molecules mediate the interaction of the PNIPAM segments with the substrate.

In addition to differences in the surface interaction in the two solvents inferred from the profile characteristics near the surface, an important difference also exists in the extension of the profiles into the subphase. The segment concentration profiles are more contracted in d-acetone than in D_2O at all temperatures as measured by the rms thickness. In particular, in all cases the diffuse layer in D_2O has a much larger dimension than the profile in d-acetone. This surprising result could indicate either a lower Flory χ parameter for a dilute brush in D_2O than in d-acetone or else a much larger statistical segment length. Regarding the former, a concentration-dependent χ could explain a low Flory χ parameter for a dilute brush as well as a cloud point for free chains in dilute solution. This is due to the fact that free chains experience much greater concentration fluctuations relative to end-tethered chains and thus would also experience greater fluctuations in the local χ. Regarding chain stiffness, Kubota has shown that in water at 20 °C PNIPAM chains behave as expanded flexible coils, using laser light scattering for fractionated PNIPAM samples of various molecular weights.[64] The same group also reported NMR data indicating a restriction of the motion of water molecules at the LCST along with an increase in the relaxation time of the side-chain protons and a sharp decrease in that of the main-chain protons. This is consistent with increased aggregation of side chains. While the precise molecular interpretation of these results is unclear, the light scattering and NMR data do not appear to support an increase in chain stiffness at the LCST sufficient to compensate for a large increase in χ. We hope to shed light on this issue with ongoing work involving PNIPAM grafted chains in which M and σ are varied independently over a wide range using atom transfer radical polymerization.[53]

In addition to these two main observations, a few other points can be made from the data. In comparing the profiles for the two tethering methods, we find that the layers are more compact (smaller rms thickness) for the "grafting-from" method. This is true in both solvents but is particularly evident in d-acetone, where a single-layer profile occurs. Notice that in Figure 5a Rq^4 for the "grafting-from" sample in d-acetone contains a sharp minimum at $q = 0.06$ Å^{-1} and rises above that in D_2O for $q > 0.08$ Å^{-1}. By contrast, in Figure 4a Rq^4 for the 220K sample in d-acetone contains a much broader minimum and remains below that in D_2O for the entire range of q examined. This corresponds to a more dense and compact profile in d-acetone for the "grafting-from" sample than for the 220K sample of method A. Since both layers have comparable dry film thicknesses this indicates that the "grafting-from" sample has a higher σ and lower M than for the 220K sample. Finally, the fact that the bilayer profile is less distinct for the "grafting-from" sample may be due to a greater polydispersity for that sample.

Conclusions

Neutron reflectivity was used to study the conformation of tethered PNIPAM chains at the interface of silicon oxide with D_2O and with d-acetone. For a wide range of M at relatively low σ, the change in conformation of tethered PNIPAM chains in D_2O was very subtle

as the temperature increased above the LCST. No coil-to-globule transition was observed. This appears to be explained by a concentration-dependent Flory χ parameter, although further measurements and theoretical analyses are needed to confirm this. Comparison of the segment profiles in d-acetone and D_2O was also revealing. A bilayer profile was obtained for the grafted PNIPAM in D_2O, composed of a thin layer of high segment volume fraction at the surface and a distinct second layer of much lower segment volume fraction extending much further into the subphase. In d-acetone, smoothly decaying single-layer profiles were obtained. The bilayer profiles in D_2O are attributed to much stronger attractive segment−surface interactions than in d-acetone due to hydrophobic interactions. Surprisingly, the PNIPAM chains are more contracted in d-acetone than in D_2O at 55 °C, despite the fact that solutions of free chains in D_2O at 55 °C are cloudy, but solutions in d-acetone are clear. This suggests a lower Flory χ parameter for a dilute brush in D_2O even above the LCST than in d-acetone. The fact that these dilute PNIPAM brushes are expanded in D_2O above the transition temperature is consistent with the very low receding water contact angles observed. This indicates that PNIPAM grafted chains at low surface density are quite hydrophilic even above the LCST.

Acknowledgment. We thank John Curro, Sergio Mendez, and Jeff Koberstein for helpful discussions. Sandia is a multiprogram laboratory operated by Sandia Corp., a Lockheed Martin Co., for the United States Department of Energy under Contract DE-AC04-94AL85000.

References and Notes

(1) Lin, S.-Y.; Chen, K.-S.; Chu, L.-R. *Polymer* **1999**, *40*, 2619.
(2) Percot, A.; Zhu, X. X.; Lafleur, M. *J. Polym. Sci., Polym. Phys.* **2000**, *38*, 907.
(3) Katsumoto, Y.; Tanaka, T.; Sato, H.; Ozaki, Y. *J. Phys. Chem. A* **2002**, *106*, 3429.
(4) Schild, H. G. *Prog. Polym. Sci.* **1992**, *17*, 163.
(5) Hirotsu, S.; Yamamoto, I.; Matsuo, A.; Okajim, T.; Furukawa, H.; Yamamoto, T. *J. Phys. Soc. Jpn.* **1995**, *64*, 2898.
(6) Hoffman, A. S. *J. Controlled Release* **1987**, *6*, 297.
(7) Stayton, P. S.; Shimoboji, T.; Long, C.; Chilkoti, A.; Chen, G.; Harris, J. M.; Hoffman, A. S. *Nature (London)* **1995**, *378*, 472.
(8) Feil, H.; Bae, Y. H.; Jan, F.; Kim, S. W. *J. Membr. Sci.* **1991**, *64*, 283.
(9) Park, Y. S.; Ito, Y.; Imanishi, Y. *Langmuir* **1998**, *14*, 910.
(10) Yamada, N.; Okano, T.; Sakai, H.; Karikusa, F.; Sawasaki, Y.; Sakurai, Y. *Makromol. Chem., Rapid Commun.* **1990**, *11*, 571.
(11) Okano, T.; Yamada, N.; Okuhara, M.; Sakai, H.; Sakurai, Y. *Biomaterials* **1995**, *16*, 297.
(12) Kawaguchi, H.; Fujimoto, K.; Mizuhara, Y. *Colloid Polym. Sci.* **1992**, *270*, 53.
(13) Okano, T.; Kikuchi, A.; Sakurai, Y.; Takei, Y.; Ogata, N. *J. Controlled Release* **1995**, *36*, 125.
(14) Ista, L. K.; Perez-Luna, V. H.; Lopez, G. P. *Appl. Environ. Microbiol.* **1999**, *65*, 2552.
(15) Chan, H. S.; Dill, K. A. *Phys. Today* **1993**, *46*, 24.
(16) Post, C. B.; Zimm, B. H. *Biopolymers* **1982**, *21*, 2139.
(17) Suzuki, A.; Tanaka, T. *Nature (London)* **1990**, *346*, 345.
(18) Zhang, J.; Pelton, R.; Deng, Y. *Langmuir* **1995**, *11*, 2301.
(19) Zhou, S.; Wu, C. *Macromolecules* **1996**, *29*, 4998.
(20) Liang, L.; Feng, X.; Liu, J.; Rieke, P. C.; Fryxell, G. E. *Macromolecules* **1998**, *31*, 7845.
(21) Wu, C.; Zhou, S. *Macromolecules* **1995**, *28*, 8381.
(22) Wang, X.; Qiu, X.; Wu, C. *Macromolecules* **1998**, *31*, 2972.
(23) Kubota, K.; Fujishige, S.; Ando, I. *J. Phys. Chem.* **1990**, *94*, 5154.
(24) Kidoaki, S.; Ohya, S.; Nakayama, Y.; Matsuda, T. *Langmuir* **2001**, *17*, 2402.
(25) Otsu, T.; Matsumoto, A. *Adv. Polym. Sci.* **1998**, *136*, 75.
(26) Zhu, P. W.; Napper, D. H. *Colloids Surf. A* **1996**, *113*, 145.
(27) Zhu, P. W.; Napper, D. H. *J. Phys. Chem. B* **1997**, *101*, 3155.
(28) Gao, J.; Wu, C. *Macromolecules* **1997**, *30*, 6873.
(29) Walldal, C.; Wall, S. *Colloid Polym. Sci.* **2000**, *278*, 936.
(30) Takei, Y.; Aoki, T.; Saui, K.; Ogata, N.; Sakurai, Y.; Okano, T. *Macromolecules* **1994**, *27*, 6163.
(31) Schmitt, F.-J.; Park, C.; Simon, J.; Ringsdorf, H.; Israelachvili, J. *Langmuir* **1998**, *14*, 2838.
(32) Halperin, A.; Tirrell, M.; Lodge, T. P. *Adv. Polym. Sci.* **1992**, *100*, 31.
(33) Kent, M. S. *Macromol. Rapid Commun.* **2000**, *21*, 243 and references therein.
(34) Baulin, V. A.; Halperin, A. *Macromol. Theory Simul.*, in press.
(35) Pincus, P. *Macromolecules* **1991**, *24*, 2912.
(36) Alexander, S. *J. Phys. (Paris)* **1977**, *38*, 977.
(37) Afroze, F.; Nies, E.; Berghmans, H. *J. Mol. Struct.* **2000**, *554*, 55.
(38) Sano, K.; Machida, S.; Sasaki, H.; Yoshiki, M.; Mori, Y. *Chem. Lett.* **1992**, 1477.
(39) Karim, A.; Satija, S. K.; Orts, W.; Ankner, J. F.; Malkrzak, C. F.; Fetters, L. J. *Mater. Res. Soc. Symp. Proc.* **1993**, *304*, 149.
(40) Luzinov, I.; Julthongpiput, D.; Liebmann-Vinson, A.; Cregger, T.; Foster, M. D.; Tsukruk, V. V. *Langmuir* **2000**, *16*, 504.
(41) Whitesell, J. K.; Chang, H. K. *Science* **1993**, *621*, 73.
(42) Wieringa, R. H.; Schouten, A. J. *Macromolecules* **1996**, *29*, 3032.
(43) Heise, A.; Menzel, H.; Yim, H.; Foster, M. D.; Wieringa, R. H.; Schouten, A. J.; Erb, V.; Stamm, M. *Langmuir* **1997**, *13*, 723.
(44) Okahata, Y.; Noguchi, H.; Seki, T. *Macromolecules* **1986**, *19*, 494.
(45) Stayton, P. S.; Shimoboji, T.; Long, C.; Chilkoti, A.; Chen, G.; Harris, J. M.; Hoffman, A. S. *Nature (London)* **1995**, *378*, 472.
(46) Certain trade names and company products are identified in order to specify adequately the experimental procedure. In no case does such identification imply recommendation or endorsement by the National Institute of Standards and Technology, nor does it imply that the products are necessarily the best for the purpose.
(47) Heise, A.; Menzel, H.; Yim, H.; Foster, M. D.; Wieringa, R. H.; Schouten, A. J.; Erb, V.; Stamm, M. *Langmuir* **1997**, *13*, 723.
(48) Baker, M. V.; Watling, J. D. *Langmuir* **1997**, *13*, 2027.
(49) Styrkas, D.; Doran, S. J.; Gilchrist, V.; Keddie, J. L.; Lu, J. R.; Murphy, E.; Sackin, R.; Su, T.-J.; Tzitzinou, A. In *Polymer Surfaces and Interfaces III*; Richards, R. W., Peace, S. K., Eds.; John Wiley & Sons Ltd.: New York, 1999.
(50) Russell, T. P. *Mater. Sci. Rep.* **1990**, *5*, 171.
(51) Smith, L.; Doyle, C.; Gregonis, D. E.; Andrade, J. D. *J. Appl. Polym. Sci.* **1982**, *26*, 1269.
(52) Lu, J. R.; Su, T. J.; Thirtle, P. N.; Thomas, R. K.; Rennie, A. R.; Cubitt, R. *J. Colloid Interface Sci.* **1998**, *206*, 212.
(53) Yim, H.; Kent, M. S.; Mendez, S.; Balamurugan, S. S.; Balamurugan, S.; Lopez, G. P. Satija, S., submitted to *Macromolecules*.
(54) Szleifier, I.; Carignano, M. A. *Adv. Chem. Phys.* **1996**, *94*, 165.
(55) Cosgrove, T.; Heath, T.; van Lent, B.; Leermakers, F.; Scheutjens, J. *Macromolecules* **1988**, *20*, 1692.
(56) Cosgrove, T. *J. Chem. Soc., Faraday Trans.* **1990**, *86*, 1323.
(57) Milner, S. T. *J. Chem. Soc., Faraday Trans.* **1990**, *86*, 1349.
(58) Grest, G. S.; Murat, M. *Macromolecules* **1993**, *26*, 3108.
(59) Atkinson, P. J.; Dickinson, E.; Horne, D. S.; Richardson, R. M. *J. Chem. Soc., Faraday Trans.* **1995**, *91*, 2847.
(60) Fragneto, G.; Thomas, R. K.; Rennie, A. R.; Penfold, J. *Science* **1995**, *267*, 657.
(61) Cosgrove, T.; Obey, T. M.; Vincent, B. *J. Colloid Interface Sci.* **1986**, *111*, 409.
(62) Yim, H.; Kent, M.; Matheson, A.; Ivkov, R.; Satija, S.; Majewski, J.; Smith, G. S. *Macromolecules* **2000**, *33*, 6126.
(63) Karim, A.; Satija, S. K.; Douglas, J. F.; Ankner, J. F.; Fetters, L. J. *Phys. Rev. Lett.* **1994**, *73*, 3407.
(64) Kubota, K.; Fujishige, S.; Ando, I. *Polym. J.* **1990**, *22*, 15.

MA021548O